

express the receptor tyrosine kinase oncoproteins RET or NTRK1 (2), follicular carcinomas express the transcription factor oncoprotein PAX8-PPAR $\gamma$ 1. This may account, at least in part, for the phenotypic and clinical differences between these two tumors.

PAX8-PPAR $\gamma$ 1 may aid in the differential diagnosis of follicular carcinomas (potentially malignant) from follicular adenomas (benign) in fine needle aspiration biopsies. This would help to reduce the number of thyroid surgeries performed, increase the percentage of malignancies resected, and reduce the costs of treating patients with thyroid nodules (20). Notably, nuclear receptor ligands for PML-RAR $\alpha$  have proven highly effective in treatment of patients with acute promyelogenous leukemia (21). It will therefore be important to determine whether ligands involving PPAR $\gamma$  pathways can benefit patients with thyroid carcinoma as an adjunct or alternative to standard surgery and radio-iodine therapy.

References and Notes

1. P. Nowell and D. Hungerford, *Science* **132**, 1497 (1960); J. Rowley, *Nature* **243**, 290 (1973); T. Rabbitts, *Nature* **372**, 143 (1994).
2. A. Fusco et al., *Nature* **328**, 170 (1987); M. Grieco et al., *Cell* **60**, 558 (1990); M. Pierotti et al., *Genes Chromosomes Cancer* **16**, 1 (1996).
3. J. Rowley, *Annu. Rev. Genet.* **32**, 495 (1998); T. Enver and M. Greaves, *Cell* **94**, 9 (1998); F. Barr, *Nature Genet.* **19**, 121 (1998); T. Rabbitts, *N. Engl. J. Med.* **338**, 192 (1998).
4. Thyroid follicular tumors were selected for this study on the basis of availability of both thyroidectomy specimens and frozen tumor tissues. The diagnoses of all thyroid tumors were rendered by staff pathologists at the Brigham and Women's Hospital or Children's Hospital, Boston, using World Health Organization and current standard practice criteria [Chr. Hedinger, *Histologic Typing of Thyroid Tumours* (Springer-Verlag, Berlin, ed. 2, 1988); J. Rosai, M. Carcangiu, R. DeLellis, *Atlas of Tumor Pathology: Tumors of the Thyroid Gland* (Armed Forces Institute of Pathology, Washington, DC, 1992)]. All follicular carcinomas, and not follicular adenomas, exhibited vascular and/or full-thickness capsular invasion by tumor cells. The follicular carcinoma patients included six adults (ages 25 to 69) and two children (ages 11 and 13) with tumors (2.2 to 6 cm) lacking local invasion or metastases.
5. L. Bondeson et al., *Cancer* **64**, 680 (1989); R. Jenkins et al., *Cancer* **66**, 1213 (1990); J. Teysseier, F. Liautaud-Roger, D. Ferre, M. Patey, J. Dufer, *Cancer Genet. Cytogenet.* **50**, 249 (1990); G. Sozzi et al., *Cancer Genet. Cytogenet.* **64**, 38 (1992); L. Roque et al., *Cancer Genet. Cytogenet.* **67**, 1 (1993); L. Roque, S. Castedo, A. Clode, J. Soares, *Genes Chromosomes Cancer* **8**, 199 (1993).
6. Interphase FISH was performed as described [S. Xiao et al., *Am. J. Pathol.* **147**, 896 (1995)], with modifications [C. Hoffman and F. Winston, *Gene* **57**, 267 (1987); D. Sinnott, C. Richer, A. Baccichet, *Biotechniques* **24**, 752 (1998)].
7. A. Mansouri, K. Chowdhury, P. Gruss, *Nature Genet.* **19**, 87 (1998).
8. RACE, RT-PCR, and Northern blots were performed with total RNA isolated from thyroid tissues by either guanidine thiocyanate-cesium chloride or by TRIzol reagent (Life Technologies). For RACE and RT-PCR, cDNA synthesis was performed on 1  $\mu$ g of total RNA at 42°C for 25 min using oligo(dT)-m13 primers (Takara, Shiga, Japan). SMART RACE was used to generate full-length PAX8-PPAR $\gamma$  cDNA clones (Clontech). 5' PAX8 primers included 5'-GCCACCAAGTCCCTGAGTCC-3', 5'-GCAT-TGACTCACAGAGCAGCA-3', 5'-GCTCAACAGCACCTT-GGA-3', 5'-GCAACTCTCGACTCACCAG-3', 5'-GAC-

- CTACGGGAGGAAGCCC-3', and 5'-GCGGACCAAG-CAGTGAG-3'. 3' PPAR $\gamma$  primers included 5'-CAAAG-GACTGGGAGTGGTCT-3', 5'-CATTACCGAGAGATCC-ACGG-3', and 5'-TTCTTATGGTCTGAGATTTCC-3'. PCR products were gel-purified and/or subcloned and sequenced using large dye terminator chemistries on automated 310 or 377 DNA sequencers (Applied Biosystems). Full-length human PPAR $\gamma$  or PAX8 cDNA probes were used for Northern blots.
9. M. Greene et al., *Gene Express.* **4**, 281 (1995); L. Fajas et al., *J. Biol. Chem.* **272**, 18779 (1997).
10. T. Kroll and J. Fletcher, unpublished data.
11. A. Poleev et al., *Development* **116**, 611 (1992); Z. Kozmik, R. Kurzbauer, P. Dorfler, M. Busslinger, *Mol. Cell. Biol.* **13**, 6024 (1993); A. Poleev et al., *Eur. J. Biochem.* **247**, 860 (1997).
12. Metabolic radiolabeling, immunoprecipitation, and SDS-polyacrylamide gel electrophoresis were performed as described [T. Kroll et al., *J. Biol. Chem.* **269**, 9270 (1994)] using Easy tag EXPRESS protein labeling mix (NEN-Dupont). Immunoprecipitations were performed with PPAR $\gamma$  mAb E8 (SC-7273) and corresponding blocking peptide (SC-7273P; both from Santa Cruz). Fibronectin was precipitated by virtue of its nonimmunospecific association with protein A-Sepharose. Primary thyroid follicular adenoma and follicular carcinoma cultures were obtained by mechanical dissociation and collagenase treatment of tumor fragments in F10 medium containing 5% fetal calf serum. Attached cells were cultured in F10 medium containing 5% fetal calf serum and mitomycin C.
13. Immunohistochemistry was performed on paraffin-embedded human thyroid tissues using microwave antigen retrieval for 30 min at 199°F in 10 mM citrate buffer, pH 6. Sections were incubated with PPAR $\gamma$  mAb E8 (12). The LSAB avidin-biotin-complex and DAB (Dako) were used for immune complex detection.
14. Transactivation assays were performed in U2OS cells as described [P. Sarraf et al., *Mol. Cell* **3**, 799 (1999)] using Eugene VI (Roche). Full-length PAX-PPAR $\gamma$ 1 cDNAs with kozak sequences were TA-cloned or ligated into the pCR3.1CMV expression vector (Invitrogen). Most experiments were performed with a

- PAX-PPAR $\gamma$ 1 form containing exons 1 to 7 plus 9 of PAX8 and exons 1 to 6 of PPAR $\gamma$ 1. The luciferase reporters were as described [R. Brun et al., *Genes Dev.* **10**, 974 (1996)]. Duplicate or triplicate samples were used for each condition; the standard deviation of the mean for all conditions was less than 20%.
15. F. Barr, *Nature Genet.* **19**, 121 (1998); T. Rabbitts et al., *Cancer Res.* **59**, 1794s (1999).
16. N. Galili et al., *Nature Genet.* **5**, 230 (1993); D. Shapiro, J. Sublett, B. Li, J. Downing, C. Naeve, *Cancer Res.* **53**, 5108 (1993); F. Barr, *Cancer Res.* **59**, 1711s (1999).
17. H. de The, C. Chomienne, M. Lanotte, L. Degos, A. Dejean, *Nature* **347**, 558 (1990); K. A. Goddard, J. Borrow, P. Freemont, E. Solomon, *Science* **254**, 1371 (1991); M. Alcalay et al., *Proc. Natl. Acad. Sci. U.S.A.* **88**, 1977 (1991); P. Pandolfi et al., *Oncogene* **6**, 1285 (1991).
18. P. Tontonoz et al., *Proc. Natl. Acad. Sci. U.S.A.* **94**, 237 (1997); P. Sarraf et al., *Nature Med.* **4**, 1046 (1998); T. Kubota et al., *Cancer Res.* **58**, 3344 (1998); E. Elstner et al., *Proc. Natl. Acad. Sci. U.S.A.* **95**, 8806 (1998); E. Mueller et al., *Mol. Cell* **1**, 465 (1998); G. Demetri et al., *Proc. Natl. Acad. Sci. U.S.A.* **96**, 3951 (1999).
19. P. Sarraf et al., *Mol. Cell* **3**, 799 (1999).
20. B. Hamberger, H. Gharib, L. Melton, J. Goellner, A. Zinsmeister, *Am. J. Med.* **73**, 381 (1988); C. Grant, I. Hay, I. Gough, P. McCarthy, J. Goellner, *Surgery* **106**, 980 (1989).
21. A. Melnick and J. Licht, *Blood* **93**, 3167 (1999).
22. T. Hudson et al., *Science* **270**, 1945 (1995); R. Gemmill et al., *Nature* **377** (suppl.), 299 (1995).
23. N. Spurr et al., *Cytogenet. Cell Genet.* **7**, 255 (1996); H. Nothwang et al., *Genomics* **41**, 370 (1997); H. Nothwang et al., *Genomics* **47**, 276 (1998).
24. We thank E. Rosen, R. Riddon, R. Shivdasani, S. Xiao, F. Moore Jr., R. Larsen, E. Cibas, C. French, J. Laguette, A. Perez-Atayde, R. Maas, D. Bowman, C. Quigley, T. Zolotarev, and the pathology resident physicians and fellows of Brigham and Women's Hospital. Supported by NIH grant CA75425 (T.G.K.).

24 January 2000; accepted 5 July 2000

## Regulated Cleavage of a Contact-Mediated Axon Repellent

Mitsuharu Hattori,\* Miriam Osterfield, John G. Flanagan†

Contact-mediated axon repulsion by ephrins raises an unresolved question: these cell surface ligands form a high-affinity multivalent complex with their receptors present on axons, yet rather than being bound, axons can be rapidly repelled. We show here that ephrin-A2 forms a stable complex with the metalloprotease Kuzbanian, involving interactions outside the cleavage region and the protease domain. Eph receptor binding triggered ephrin-A2 cleavage in a localized reaction specific to the cognate ligand. A cleavage-inhibiting mutation in ephrin-A2 delayed axon withdrawal. These studies reveal mechanisms for protease recognition and control of cell surface proteins, and, for ephrin-A2, they may provide a means for efficient axon detachment and termination of signaling.

Repulsion by direct cell contact is one of the basic mechanisms of axon guidance (1) and allows patterning of neural connections in a spatially precise manner (2, 3). However, this mechanism raises inherent questions. The binding of an axonal receptor to its cell surface ligand would be expected to favor adhesion, so how is this reconciled with repulsion? Also,

how is contact-mediated repellent signaling terminated? These questions are further emphasized by the known properties of the ephrins, which are well-characterized cell surface axon repellents: The ephrins and their receptors are expressed at high density; the receptors do not appear to be down-regulated upon ligand binding; and the receptor-ligand interaction is mul-

tivalent, has a low off rate, and has a high affinity (2–5). Despite this, axon detachment and termination of signaling presumably have to be efficient because axons explore their embryonic environment in a dynamic fashion, involving both advances and withdrawals (6–8). One potential mechanism to reconcile contact-mediated signaling with repulsion could be the cleavage of ligand from the cell surface. However, because soluble truncated forms of ephrins cannot activate their receptors (9), unregulated cleavage could create problems of its own by destroying active ligand.

Many cell surface proteins undergo ectodomain shedding by proteolytic cleavage. Examples are the liberation of signaling molecules that are active in soluble forms, such as transforming growth factor- $\alpha$ , tumor necrosis factor- $\alpha$  (TNF- $\alpha$ ), kit ligand, and Delta; adhesion molecule shedding; and shedding of the amyloid precursor protein (APP) implicated in Alzheimer's disease (10–12). ADAMs (a disintegrin and a metalloprotease) are proteases responsible for many of these shedding processes (13–15). ADAMs themselves are important for development, and Kuzbanian/ADAM10 (Kuz) was identified in a *Drosophila* genetic screen as being required for normal axon extension (16). Despite rapid progress in identifying roles for the ADAMs, their regulation and ligand specificity are not well understood. Several treatments, such as protein kinase C (PKC) activators or calcium ionophores, are known to activate generalized shedding, though it is less clear whether the known pathways can target individual substrates without activating more general proteolysis. Also, there is very little sequence specificity at the substrate cleavage sites, and it is unclear how ADAM proteases specifically recognize their correct targets. In addition to a protease domain, ADAMs have disintegrin, cysteine-rich, and cytoplasmic domains, suggesting that these other domains might function in substrate binding (13, 14).

To investigate whether ephrin-A2, a membrane-bound protein with a glycosyl-phosphatidylinositol (GPI) lipid anchor, is cleaved from the membrane, we tested the effect of a soluble EphA3 receptor ectodomain fused to an immunoglobulin Fc tag (EphA3-Fc). When Neuro2a neuroblastoma cells expressing transfected ephrin-A2 were treated with clustered EphA3-Fc, ephrin-A2 disappeared from the cell membrane fraction, and a smaller form appeared in the supernatant (Fig. 1A). Unclustered EphA3-Fc had no effect. This result indicated ephrin-A2 is cleaved from the cell membrane in a mecha-

nism regulated by binding to clustered receptor.

In time course experiments, no cleavage was seen until ~10 min after EphA3-Fc addition, and cleavage was largely complete within 45 min (Fig. 1B). The molecular size of the released product is smaller than the soluble form released by phosphatidylinositol-specific phospholipase C (PI-PLC) by ~1.9 kD (Fig. 1C), indicating that ephrin release was not due to phospholipase C or D activity and was due to cleavage within the polypeptide (17). Receptor-activated release of ephrin-A2 also occurred in NG 108 neuroblastoma cells, HEK 293T kidney epithelial cells, and NIH-3T3 embryonic fibroblasts (18), as well as in primary cultured neurons from embryonic day 18 (E18) mouse midbrain (Fig. 1D), a cellular context where ephrin-A2 and -A5 are known to function in axon guidance (2, 3, 19, 20). No cleavage activation was seen when ephrin-A2 was clustered by antibody (antibody to myc tag and secondary clustering antibody) (18), suggesting that clustering is not sufficient to activate cleavage and that EphA3-Fc may induce a specific regulatory conformational change.

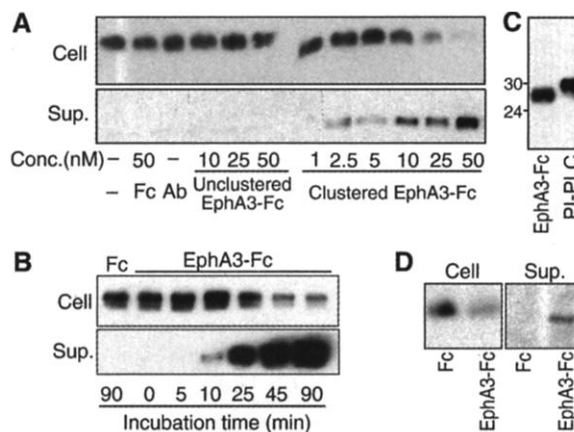
The ADAM metalloprotease Kuz shows an axon-guidance phenotype in *Drosophila* (16), has been implicated in ectodomain shedding (13, 14), and is expressed in mammalian neural cell lines (21). To assess its expression pattern in mammalian development, we performed *in situ* hybridization, showing that Kuz RNA was widely expressed in the nervous system of E18 mouse embryos, with high expression in the posterior midbrain, which diminished toward the anterior midbrain (Fig. 2B). This pattern is reminiscent of the graded midbrain expression of ephrin-A2 and -A5 (Fig. 2B) (19, 20). The cleavage of ephrin-A2 induced by EphA3-Fc was blocked by the metalloprotease inhibitor *o*-phenanthroline (Fig. 2A). A dominant negative version of Kuz (Kuz-DN) lacking the protease domain (12, 22) inhibited ephrin-A2 ectodomain shedding (Fig. 2C). Conversely,

full-length Kuz (Kuz-FL) activated shedding (Fig. 2D). These results indicate that ephrin-A2 cleavage can be mediated by an ADAM protease and suggest that Kuz is a good candidate for a role in this process during development.

Although it has been proposed that ADAM proteases might form a stable complex with the substrate to be cleaved, such a complex has not been reported (13, 14). Co-immunoprecipitation from transfected cells revealed that a complex was formed between ephrin-A2 and Kuz (Fig. 2E). This complex was seen under conditions where lipid rafts would be disrupted (23), and placental alkaline phosphatase (AP), which, like ephrin-A2, is a GPI-anchored protein, showed no coprecipitation with Kuz (Fig. 2E). The complex of ephrin-A2 and Kuz was seen in the absence of EphA3-Fc. The addition of clustered EphA3-Fc did not cause any short-term modulation of the complex (Fig. 2E), although after longer periods of time, less complex was detected as ephrin-A2 was cleaved (18). The association was not dependent on the protease domain of Kuz, because Kuz-DN, which lacks the prodomain and protease domain, still associated with ephrin-A2 (Fig. 2F). Furthermore, although Kuz-DN associated efficiently with ephrin-A2, it formed no detectable association with AP-ephrin-A2<sup>JM</sup>, a protein containing the juxtamembrane region of ephrin-A2 but excluding the receptor-binding core region (Figs. 2F and 3A), indicating that complex formation involves sequences outside the juxtamembrane cleavage region. The complex of ephrin-A2 with Kuz could involve direct or indirect binding.

A motif search with the MEME program (24) was applied to see if proteins that are cleaved by Kuz might have common sequences. A conserved motif was found in all of the proteins tested, including all eight vertebrate ephrins, Delta, TNF- $\alpha$ , and APP (Fig. 2G). This conserved motif is located roughly in the middle of the receptor-binding core domain of the ephrins. A 15-amino acid oligomer synthetic

**Fig. 1.** Clustered EphA3-Fc activates cleavage of ephrin-A2. **(A)** Neuro-2a cells expressing mouse ephrin-A2 (33) were incubated with no addition or with clustered EphA3-Fc, clustered control Fc tag (Fc), unclustered EphA3-Fc, antibody (Ab), or antibody-clustered EphA3-Fc. Cell lysate (Cell) and culture supernatant (Sup.) were collected after 2 hours and analyzed by immunoblotting with antibody to ephrin-A2 (38). Ephrin-A2 cleavage was activated by clustered EphA3-Fc. **(B)** Time course of ephrin-A2 release after the addition of clustered EphA3-Fc, 20 nM. Cleavage was first detectable by 10 min and was largely complete by 45 min. **(C)** Molecular weight (as kD) of ephrin-A2 released by clustered EphA3-Fc stimulation. The product was smaller than that released by PI-PLC (17). **(D)** Clustered EphA3-Fc-activated cleavage of ephrin-A2 was observed in primary cultured mouse E18 posterior midbrain neurons.



Department of Cell Biology and Program in Neuroscience, Harvard Medical School, 240 Longwood Avenue, Boston, MA 02115, USA.

\*Present address: Department of Molecular Neurobiology, Institute of Medical Science, University of Tokyo, Minato-ku, Tokyo, Japan.

†To whom correspondence should be addressed. E-mail: flanagan@hms.harvard.edu

REPORTS

peptide containing the sequence in ephrin-A2 activated ephrin-A2 shedding up to five times that of a scrambled-sequence peptide or no peptide. Some activation was seen in the absence of EphA3-Fc, and there was a further synergistic activation when the peptide was added together with EphA3-Fc (Fig. 2H). The effect of this peptide might involve interaction with ephrin-A2, metalloprotease, or a separate protein that could mediate their interaction. Because this motif is in the middle of the receptor-binding domain, it could be involved in the mechanism of receptor-induced cleavage activation.

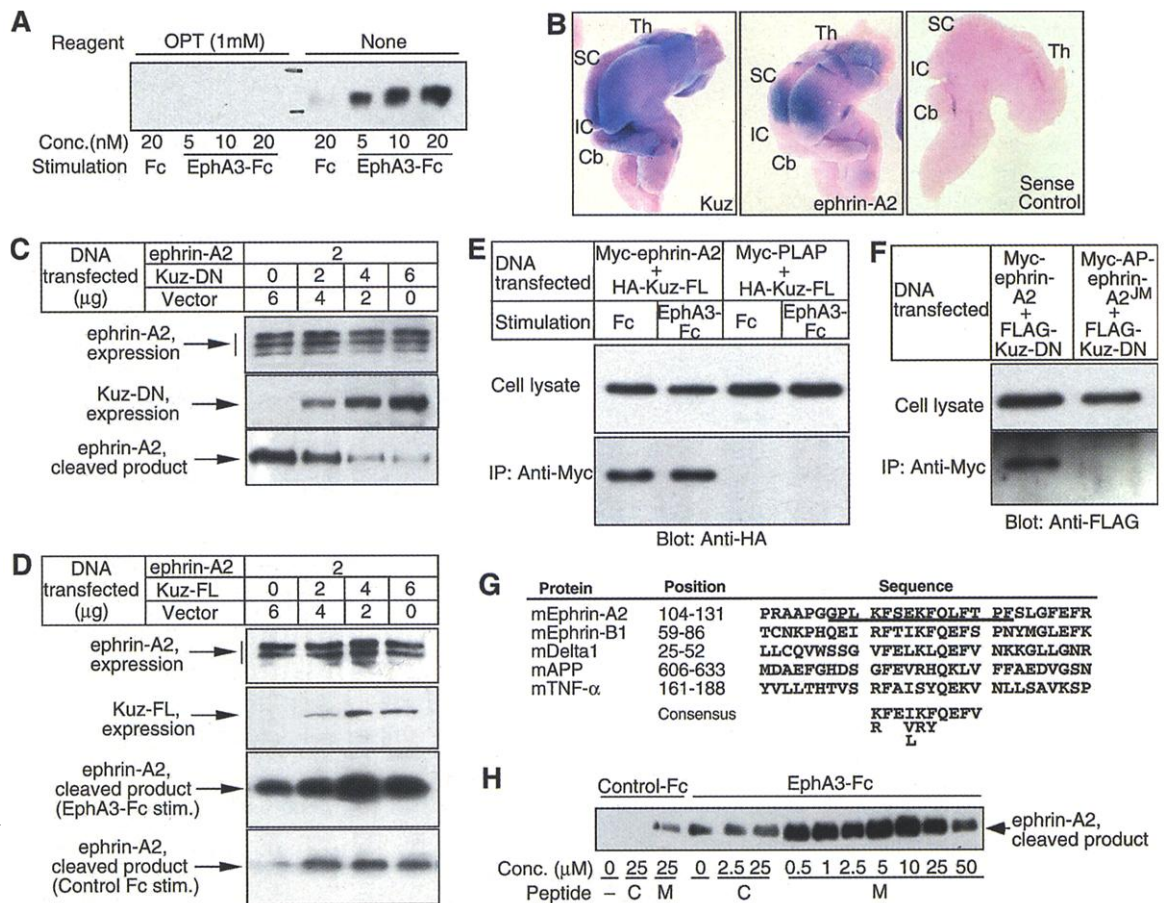
Several agents, such as PKC activators, calcium ionophores, or tyrosine phosphatase inhibitors, induce a generalized ectodomain shedding (10, 11). Also, several leukocyte surface markers are down-regulated after leukocyte ac-

tivation or antibody cross-linking, although the effect of cognate biological ligands and the specificity of this process is unclear (25–27). To assess whether the cleavage of ephrin-A2 induced by EphA3-Fc receptor is specific to the cognate ligand, we first tested for cross-activation of cleavage of the AP–ephrin-A2<sup>JM</sup> fusion protein (Fig. 3A). Although native placental AP was not shed by stimulation with the PKC activator phorbol myristate acetate (PMA), the presence of the ephrin-A2 juxtamembrane region in AP–ephrin-A2<sup>JM</sup> allowed cleavage in response to PMA (Fig. 3B). However, when ephrin-A2 cleavage was activated by EphA3-Fc, cleavage of coexpressed AP–ephrin-A2<sup>JM</sup> was not cross-activated (Fig. 3B). Likewise, EphA3-Fc activation of ephrin-A2 cleavage failed to activate cleavage of coexpressed ephrin-B1, which does not bind EphA3, even

though ephrin-B1 cleavage was efficiently activated by PMA (18). To further assess specificity, we labeled cell surface proteins of Neuro2a cells with sulfo-NHS-biotin (NHS, *N*-hydroxysuccinimide) before treatment with EphA3-Fc. Cleaved ephrin-A2 appeared in the supernatant, but no other biotin-labeled cleavage products were evident, indicating that there was not a generalized activation of ectodomain shedding (Fig. 3C).

To investigate whether ephrin-A2 shedding is limited to sites of cell-cell contact, we made a fusion protein that was composed of green fluorescent protein and ephrin-A2 (GFP–ephrin-A2) (Fig. 3A). GFP–ephrin-A2 retained the ability to bind EphA3 receptor (18) and was expressed over the entire surface of transfected cells (Fig. 3D). These cells were challenged with axons of

**Fig. 2.** Interactions of ephrin-A2 and metalloprotease. **(A)** OPT, a zinc chelator that inhibits metalloprotease action, blocked the cleavage activation of ephrin-A2 by clustered EphA3-Fc. **(B)** Whole-mount RNA in situ hybridization of E18 mouse brain; the cortex has been removed to uncover the midbrain. Probes were Kuz or ephrin-A2 antisense RNA or were Kuz sense control. SC, midbrain superior colliculus; IC, midbrain inferior colliculus; Cb, cerebellum; and Th, thalamus. Kuz expression was widespread in the nervous system and was particularly prominent in the posterior midbrain, including the posterior SC, where ephrin-A2 is most prominent, and the IC, where ephrin-A5 (3) is most prominent. **(C and D)** The effect on receptor-activated ephrin-A2 cleavage of Kuz-DN, lacking the protease domain, or Kuz-FL. NIH 3T3 cells were transfected with the plasmids indicated; DNA amounts are shown in  $\mu\text{g}$ . Cleavage of ephrin-A2 was assayed 48 hours after transfection (38). Kuz-DN inhibited the receptor-induced ectodomain shedding of ephrin-A2, whereas Kuz-FL augmented it. stim., stimulation. **(E)** Ephrin-A2 and Kuz-FL form a stable complex. Stimulation with clustered EphA3-Fc was for 15 min. The complex of ephrin-A2 and Kuz was not dependent on the addition of clustered EphA3-Fc. GPI-anchored native placental AP (PLAP) was used as a negative control. IP, immunoprecipitation. **(F)** The complex of ephrin-A2 and Kuz involves sequences outside the juxtamembrane and protease domains, respectively. Ephrin-A2 formed a complex with Kuz-DN, lacking the protease domain. AP–ephrin-A2<sup>JM</sup>, containing the entire ephrin-A2 juxtamembrane domain, formed no detectable complex. **(G)** A conserved



motif found in proteins whose cleavage can be mediated by Kuz (37). A single motif in all vertebrate ephrins and the other proteins shown was identified with the MEME program (24). The stretch of 10 amino acids showing the strongest conservation is demarcated by spaces. The 15-amino acid oligomer peptide sequence in ephrin-A2 used to make a synthetic peptide is underlined. **(H)** The ephrin-A2 cleavage assay was performed with the indicated concentrations of synthetic peptide. M, 15-amino acid oligomer peptide consisting of a motif derived from ephrin-A2, underlined in **(G)**; C, a scrambled peptide with the same amino acid composition, TEFFPPGKKLQFFSL. The ephrin-A2 15-amino acid oligomer activated ephrin-A2 cleavage in the absence of EphA3-Fc and caused, with a peak of activity at  $\sim 10 \mu\text{M}$ , a synergistic activation of cleavage in the presence of EphA3-Fc.

medial hippocampal neurons, which are repelled by ephrin-A2 (28, 29) and can be grown easily as a dispersed culture and observed in real time. Where cells expressing GFP-ephrin-A2 were contacted by an axon, fluorescence dispersed locally from the target cell surface and was seen over the axon and surrounding area (Fig. 3, D to F). However, there was no indication of a generalized dispersal of fluorescence from the rest of the cell.

Although PMA can activate ephrin-A2 cleavage, a strong PKC inhibitor, H-7, did not inhibit cleavage activated by EphA3-Fc (Fig. 3G), indicating that the receptor-regulated mechanism does not involve PKC activation. In contrast, protein tyrosine kinase inhibitors, such as genistein and herbimycin-A, did inhibit EphA3-Fc activation of cleavage (Fig. 3H). PP2, an inhibitor specific for Src-family kinases (30), had no obvious effect, however. These results appear consistent with the ability of vanadate, a tyrosine phosphatase inhibitor, to cause a general activation in cleavage of surface proteins (31), including ephrin-A2 (18), indicat-

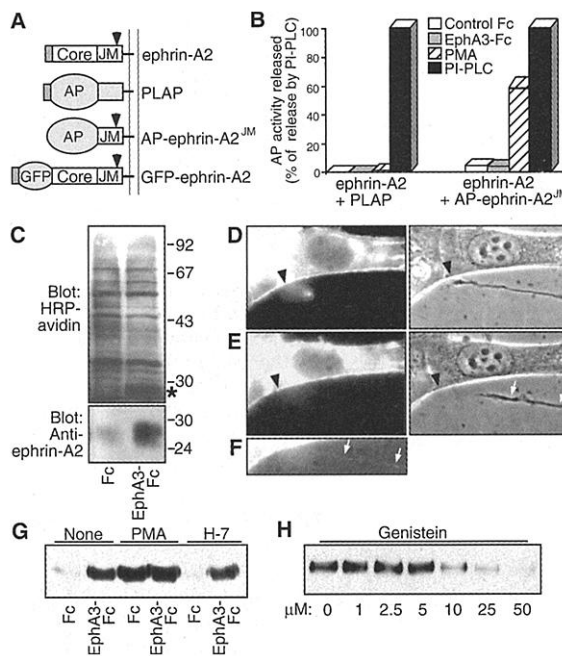
ing that tyrosine kinases are either involved in or can modulate the receptor-induced pathway of ephrin cleavage.

To determine whether ephrin-A2 cleavage affects axon behavior, we created a proteolysis-blocking mutation in ephrin-A2. As with other proteins that undergo ectodomain shedding, point mutations, insertions, or deletions in the juxtamembrane region of ephrin-A2 typically had little or no effect on cleavage. However, two constructs, ephrin-A2<sup>IS2</sup> and ephrin-A2<sup>IS3</sup>, which have a short insertion in the juxtamembrane region (Fig. 4A), were not cleaved by EphA3-Fc stimulation or PKC activation, although their binding affinity for the EphA3 receptor was unaffected (Fig. 4B) (18). Stable transformant cells expressing wild-type or un-cleavable ephrin-A2<sup>IS3</sup> were isolated. These lines showed similar ephrin-A2 protein expression, and doxycycline removal allowed expression levels to be induced and controlled (32, 33). Axon responses to these target cells were assessed by using medial hippocampal neurons. "Growth cone collapse" was defined as full collapse with no obvious growth cone structure

remaining, and "withdrawal" was defined as no discernible connection between axon and target cell. Cells that did not express ephrin-A ligands caused no growth cone collapse ( $n = 10$  axon trials). Upon ephrin expression, both the ephrin-A2 and ephrin-A2<sup>IS3</sup> cell lines caused growth cone collapse within 10 min of first contact ( $n = 21$  axons in each group). With wild-type ephrin-A2, axon withdrawal followed growth cone collapse with an average time of  $26.6 \pm 14.8$  min (mean  $\pm$  SD) (Fig. 4, C, E, and F). With ephrin-A2<sup>IS3</sup> cells, axon withdrawal was greatly delayed, with an average time of  $72.5 \pm 36.0$  min ( $P < 0.0001$ , unpaired  $t$  test) (Fig. 4, D to F). In about half of these cases, the axon remained collapsed and stuck to the target cell for over 80 min (Fig. 4, D and E), whereas all of the control axons had withdrawn by this time (Fig. 4, C and E). It is unlikely that the differences in time course can be explained by the expression level of ephrin-A2, because doxycycline modulation of the expression levels over a several-fold concentration range had no discernible effect on axon withdrawal (18). A delay was seen even when the initial contact leading to collapse involved only one to three filopodia (wild-type ephrin-A2,  $n = 10$ ,  $30.3 \pm 15.1$  min; ephrin-A2<sup>IS3</sup>,  $n = 9$ ,  $73.9 \pm 29.9$  min;  $P < 0.005$ ) (Fig. 4F) and similarly when it was more extensive (wild-type ephrin-A2,  $n = 8$ ,  $26.1 \pm 16.4$  min; ephrin-A2<sup>IS3</sup>,  $n = 11$ ,  $64.8 \pm 36.0$  min;  $P < 0.01$ ). The kinetics of growth cone collapse and withdrawal when wild-type ephrin-A2 was used in this assay appear consistent with the rate of ephrin-A2 cleavage induced by clustered EphA3-Fc, especially considering that the rate of receptor-ligand association has to be factored into the EphA3-Fc experiments. The kinetics also appear comparable to real-time studies of axon behavior in vivo [for example, (6, 8)] as well as to ephrin-mediated withdrawal induced by primary cultured neurons or glia in vitro (34). Our results show that a mutation that blocks ephrin cleavage does not prevent signaling leading to growth cone collapse but does inhibit axon withdrawal. Because growth cones never recovered from collapse while they remained bound to a target cell (Fig. 4D), the cleavage-inhibiting mutation evidently interferes with their ability to terminate ephrin signaling. In addition, because axons can withdraw rapidly in response to soluble clustered ephrin-Fc protein (35) or membrane suspensions bearing ephrins, including ephrin-A2<sup>IS3</sup> (18, 36), it is likely that at least part of the delay in withdrawal seen here with intact target cells is due to an impairment of axon detachment.

A stable complex formed by ADAM protease and ephrin in the absence of Eph receptor is likely to play a role in the specificity of protease-substrate recogni-

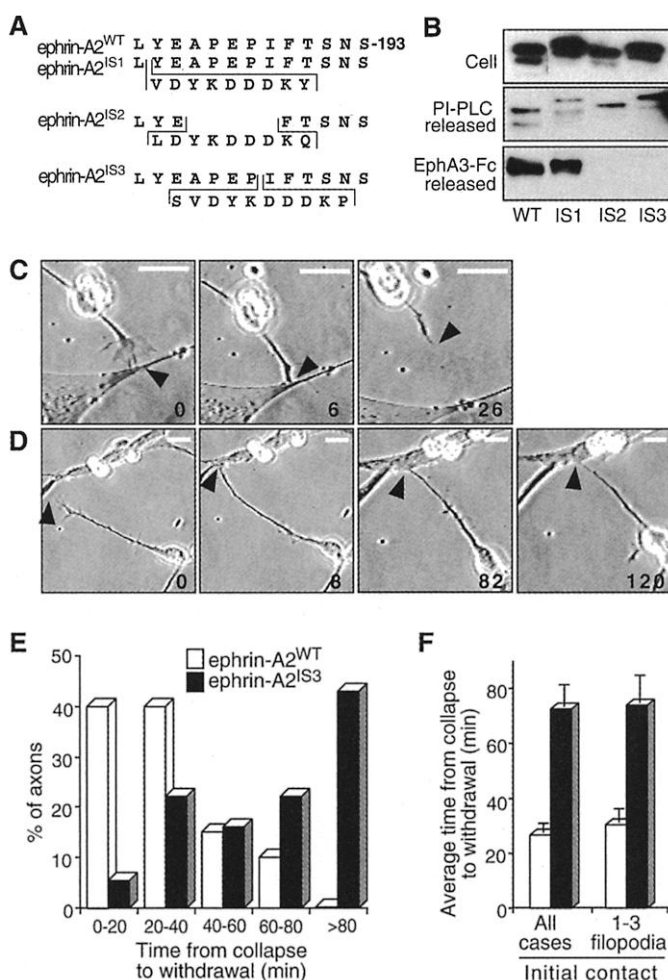
**Fig. 3.** Receptor activation of ephrin-A2 cleavage is not accompanied by general cleavage of membrane proteins and is blocked by protein tyrosine kinase inhibitors. (A) Schematic diagram of ephrin-A2 constructs (33). Core, receptor-binding core domain conserved throughout the ephrin family; JM, juxtamembrane domain of ephrin-A2 with arrowhead denoting the cleavage site; AP, alkaline phosphatase; and GFP, green fluorescent protein. The horizontal line denotes the GPI membrane anchor, and the dark boxes indicate myc epitope tags. (B) The indicated plasmids were transfected into NIH-3T3 cells and incubated for 2 hours with clustered control-Fc (open bar), clustered EphA3-Fc (shaded bar), 1  $\mu$ M PMA (hatched bar), or PI-PLC (solid bar). Culture supernatants were collected, and AP activity was quantitated. Clustered EphA3-Fc treatment activated cleavage of ephrin-A2 but not coexpressed AP-ephrin-A2<sup>JM</sup>. (C)



Neuro-2a cells expressing mouse ephrin-A2 were surface labeled with sulfo-NHS-biotin (0.2 mg/ml for 30 min at 4°C in PBS) and stimulated with either clustered control Fc or clustered EphA3-Fc. Culture supernatants were blotted with HRP-streptavidin (upper panel) or anti-ephrin-A2 (lower panel). Clustered EphA3-Fc induced ephrin-A2 release (lower panel), and a band at the size of ephrin-A2 is visible in the sulfo-NHS-labeled fraction (asterisk in upper panel), but generalized ectodomain shedding was not seen. Molecular weights are shown as kD. (D to F) Localized shedding of GFP-ephrin-A2 fluorescence. Fluorescence micrographs are on the left, and phase-contrast images are on the right (39). The paired images were taken within 30 s, although they are not precisely superimposable because of axon motility. At the site of axonal contact (black arrowhead), there was a localized dispersal of fluorescence from the target cell, seen in (D) at approximately the time of growth cone collapse. As the axon withdrew 15 min later (E), the dispersed fluorescence was no longer easily seen. However, in a brighter version of the same image (F), faint staining could be seen over the axon (white arrows); this was not seen in axons that had not contacted a fluorescent cell. (G) PMA (1  $\mu$ M), an activator of PKC, activates cleavage of ephrin-A2. However, H-7 (20  $\mu$ M), a powerful inhibitor of PKC, does not suppress the receptor-induced cleavage of ephrin-A2 caused by clustered EphA3-Fc. (H) Genistein, a protein tyrosine kinase inhibitor, suppressed the receptor-induced activation of ephrin-A2 cleavage caused by clustered EphA3-Fc.

REPORTS

**Fig. 4. Uncleavable mutant of ephrin-A2 delays axon withdrawal.** (A) Amino acid sequence of ephrin-A2 insertion mutants (37). Inserted sequences are in brackets. All constructs here, including the wild-type sequence, were myc epitope tagged at the NH<sub>2</sub>-terminus (33). (B) To test for cleavage, we transfected the mutant plasmids into NIH-3T3 cells and challenged them with EphA3-Fc. The ephrin-A2<sup>IS1</sup> insertion mutant, as well as several point mutants and deletions not shown here, was still cleaved. However, ephrin-A2<sup>IS2</sup> and ephrin-A2<sup>IS3</sup> were not detectably cleaved. WT, wild type. (C and D) Time-lapse videomicroscopy (39) of typical mouse hippocampal neurons contacting TetOff cells that were stably transfected with ephrin-A2 (C) or ephrin-A2<sup>IS3</sup> (D). Time is given in minutes from the first contact. In (C), the neuronal growth cone collapsed by 6 min and had fully withdrawn by 26 min; in (D), the growth cone collapsed by 8 min and remained collapsed but had not withdrawn from the target cell by 120 min. Scale bars, 25 μm. (E and F) Histograms of the interval between the times of growth cone collapse and axon withdrawal. Open bars indicate ephrin-A2-expressing cells, and solid bars indicate ephrin-A2<sup>IS3</sup>-expressing cells. (E) Axons were divided into five groups with different withdrawal times. (F) Mean withdrawal times (error bars show standard errors) for all axons and for the subset of axons where the initial contact leading to collapse involved only one to three filopodia. The ephrin-A2<sup>IS3</sup> mutation delayed axon withdrawal.



tion, as well as in enhancing the efficiency and localization of subsequent cleavage. The triggering of proteolytic activity by clustered receptor provides a mechanism to tightly coordinate cleavage with repulsion, because Eph receptor signaling is triggered by clustered ligand. The specificity of the receptor-activated cleavage mechanism for the cognate ligand provides a way to limit cleavage to molecules at the site of cell-cell contact, thus allowing the target cell to retain its repellent properties, sparing other cell surface proteins. The proposed mechanism can also account for the termination of repellent signaling because truncated soluble ephrins fail to activate Eph receptors (9). In addition to axon repulsion, the cleavage mechanism described here could be involved in contact-mediated axon attraction by ephrins or other molecules and could potentially provide a way to control

whether cell contacts are repellent or adhesive. The regulatory mechanisms described here may also provide new ways to understand or manipulate other cleavage events mediated by ADAM proteases with roles in development, physiology, and disease.

References and Notes

1. M. Tessier-Lavigne and C. S. Goodman, *Science* **274**, 1123 (1996).
2. J. G. Flanagan and P. Vanderhaeghen, *Annu. Rev. Neurosci.* **21**, 309 (1998).
3. U. Drescher, F. Bonhoeffer, B. Muller, *Curr. Opin. Neurobiol.* **7**, 75 (1997).
4. N. W. Gale and G. D. Yancopoulos, *Cell Tissue Res.* **290**, 227 (1997).
5. M. Lackmann et al., *J. Biol. Chem.* **272**, 16521 (1997).
6. P. Godement, L. C. Wang, C. A. Mason, *J. Neurosci.* **14**, 7024 (1994).
7. H. Nakamura and D. M. O'Leary, *J. Neurosci.* **9**, 3776 (1989).
8. M. J. Murray and P. M. Whittington, *J. Neurosci.* **19**, 7901 (1999).
9. S. Davis et al., *Science* **266**, 816 (1994).

10. J. Massague and A. Pandiella, *Annu. Rev. Biochem.* **62**, 515 (1993).
11. N. M. Hooper, E. H. Karran, A. J. Turner, *Biochem. J.* **321**, 265 (1997).
12. H. Qi et al., *Science* **283**, 91 (1999).
13. J. Schlondorff and C. P. Blobel, *J. Cell Sci.* **112**, 3603 (1999).
14. P. Primakoff and D. G. Myles, *Trends Genet.* **16**, 83 (2000).
15. Z. Werb and Y. Yan, *Science* **282**, 1279 (1998).
16. D. Fambrough, D. J. Pan, G. M. Rubin, C. S. Goodman, *Proc. Natl. Acad. Sci. U.S.A.* **93**, 13233 (1996).
17. Apparent molecular weights of PI-PLC-cleaved and EphA3-Fc-induced cleavage products of ephrin-A2 were estimated at 30.6 and 28.7 kD, respectively. This size difference is not consistent with cellular phospholipase C or D action. Considering that the molecular weight of the PI-PLC-cleaved glycan structure is ~1 to 1.5 kD, the cleavage site is estimated to be between Pro<sup>187</sup> and Ser<sup>193</sup>.
18. M. Hattori, M. Osterfield, J. G. Flanagan, data not shown.
19. J. Frisén et al., *Neuron* **20**, 235 (1998).
20. D. A. Feldheim et al., *Neuron* **25**, 563 (2000).
21. R. Yavari, C. Adida, P. Bray-Ward, M. Brines, T. Xu, *Hum. Mol. Genet.* **7**, 1161 (1998).
22. D. J. Pan and G. M. Rubin, *Cell* **90**, 271 (1997).
23. At 24 to 36 hours after transfection, cells were washed with cold phosphate-buffered saline (PBS) and lysed in RIPA114 buffer [50 mM tris (pH 8.0), 100 mM NaCl, 5 mM EDTA, 1% Triton-X114, and 0.2% SDS] for 2 hours at 4°C and then centrifuged at 14,000 rpm for 10 min at 4°C. This provides a stronger detergent than Triton-X100 or NP-40, solubilizing lipid rafts. The complex of Kuz and ephrin-A2 was also seen in 0.9% Brij96, another detergent that solubilizes rafts. The supernatant was mixed with precipitating antibody at a final concentration of 2 μg/ml and rotated for 1 hour at 4°C. Protein A-Sepharose beads (Amersham Pharmacia) were added, and after rotating for another hour at 4°C, the beads were washed with RIPA114 buffer four times and analyzed by SDS-polyacrylamide gel electrophoresis (SDS-PAGE) and immunoblotting.
24. W. N. Grundy, T. L. Bailey, C. P. Elkan, *Comput. Appl. Biosci.* **12**, 303 (1996); <http://meme.sdsc.edu>.
25. C. Feehan et al., *J. Biol. Chem.* **271**, 7019 (1996).
26. M. Wroblewski and A. Hamann, *Int. Immunol.* **9**, 555 (1997).
27. V. V. Swarte, D. H. Joziassse, R. E. Mebius, D. H. van den Eijnden, G. Kraal, *Cell Adhes. Commun.* **6**, 311 (1998).
28. P. P. Gao et al., *Proc. Natl. Acad. Sci. U.S.A.* **93**, 11161 (1996).
29. J. H. Zhang, D. P. Cerretti, T. Yu, J. G. Flanagan, R. Zhou, *J. Neurosci.* **16**, 7182 (1996).
30. A. Davy et al., *Genes Dev.* **13**, 3125 (1999).
31. M. Vecchi, L. A. Rudolph-Owen, C. L. Brown, P. J. Dempsey, G. Carpenter, *J. Biol. Chem.* **273**, 20589 (1998).
32. P. Shockett, M. Difilippantonio, N. Hellman, D. G. Schatz, *Proc. Natl. Acad. Sci. U.S.A.* **92**, 6522 (1995).
33. An ephrin-A2 expression plasmid was made by ligating mouse ephrin-A2 cDNA between the Hind III and Xho I sites of pSecTag2A (Invitrogen) and inserting a myc epitope tag oligonucleotide between the Sfi I and Hind III sites, just after the secretion signal peptide. Mutant ephrin-A2 plasmids were produced by modifying this construct, and GFP-ephrin-A2 was made by inserting EGFP (Clontech) and an eight-amino acid linker, SSGGSGL, after the myc epitope (37). To make AP-ephrin-A2JM, we amplified the entire juxtamembrane protein-coding sequence between Val<sup>164</sup> and the stop codon of mouse ephrin-A2 by polymerase chain reaction, ligated the sequence between the Xho I and Xba I sites of pAptag-5 (GenHunter, Nashville, TN), and inserted a myc epitope tag oligonucleotide between the Sfi I and Hind III sites. For Kuz constructs, the coding region of mouse Kuz cDNA was ligated into pSecTag2A, and hemagglutinin (HA) or FLAG epitope sequences were added to the intracellular COOH-terminus. To make doxycycline-repressible constructs, we transferred myc-tagged ephrin-A2 cDNAs from pSecTag2A into pTRE (Clontech).

34. R. W. Davenport, E. Thies, R. Zhou, P. G. Nelson, *J. Neurosci.* **18**, 975 (1998).
35. L. Meima *et al.*, *Eur. J. Neurosci.* **9**, 177 (1997).
36. E. C. Cox, B. Müller, F. Bonhoeffer, *Neuron* **2**, 31 (1990).
37. Single-letter abbreviations for the amino acid residues are as follows: A, Ala; C, Cys; D, Asp; E, Glu; F, Phe; G, Gly; H, His; I, Ile; K, Lys; L, Leu; M, Met; N, Asn; P, Pro; Q, Gln; R, Arg; S, Ser; T, Thr; V, Val; W, Trp; and Y, Tyr.
38. Cells were washed twice with culture medium, and control Fc or EphA3-Fc protein was added for 2 hours unless otherwise stated. These Fc proteins were preclustered with polyclonal antibody to human Fc (Jackson ImmunoResearch, West Grove, PA) for 30 min on ice. Midbrain neurons were cultured on laminin/poly-L-lysine-coated dishes for 3 days before the cleavage assay in Neurobasal/B27 medium (Gibco). After incubation, the cells were collected in SDS-PAGE sample buffer. The culture supernatant was spun at 14,000 rpm for 10 min at 4°C, then protein was precipitated with trichloroacetic acid and dis-

- solved in SDS-PAGE sample buffer, adjusting the pH with 1M NaOH. For ephrin-A2 immunoblots, polyvinylidene difluoride membranes were probed with rabbit anti-ephrin-A2 (Santa Cruz Biotechnology) diluted 1:1500, and the secondary antibody was horseradish peroxidase (HRP)-conjugated sheep anti-rabbit immunoglobulin G (IgG) (Amersham Pharmacia Biotech) diluted 1:2000, with detection by an enhanced chemiluminescence kit. Epitope tags were detected with antibody to Myc 9E10 (100 ng/ml), antibody to Flag F2 (200 ng/ml), or antibody to HA 3F10 (50 ng/ml), with HRP-conjugated sheep anti-mouse IgG secondary antibody diluted 1:3500.
39. Videomicroscopy was as follows. Cultures were on 25-mm glass coverslips that were precoated overnight with mouse laminin (2 µg/ml). Ephrin-A2 plasmids were stably transfected into NIH-3T3 fibroblasts, and before the assay, these cells were plated at  $0.5 \times 10^5$  to  $2 \times 10^5$  cells/ml in Dulbecco's modified Eagle's medium with 10% calf serum. The medial half of the hippocampus was removed from E16 to E18 mice, dissociated in neurobasal/B27 me-

- dium, and plated between  $10^4$  and  $10^6$  cells/ml to obtain a good density for observation. After culturing for 16 to 40 hours, coverslips were viewed with a Zeiss Axiovert microscope and a charge-coupled device camera, with the stage warmed to 37°C, and 20 mM Hepes was added to the medium to maintain pH at ~7.4. Single-axon growth cones approaching a target cell were recorded every 30 s with phase-contrast optics. For GFP experiments, one to four images were recorded with fluorescein optics. All results were confirmed blind by an independent investigator.
40. We thank L. Ma, R. Davis, T. Inoue, T. Wei, D. Marks, D. Feldheim, Q. Lu, M. Kirschner, B. Freeman, D. Van Vactor, and K. Mikoshiba for help and discussions and D. Pan for mouse Kuz plasmids. This work was supported by a fellowship from the Society for Promotion of Arts and Science of Japan (M.H.) and by NIH grants HD29417 and EY11559 and a fellowship from the Klingenstein foundation (J.G.F.).

16 February 2000; accepted 15 June 2000

## Function of an Axonal Chemoattractant Modulated by Metalloprotease Activity

Michael J. Galko and Marc Tessier-Lavigne\*

The axonal chemoattractant netrin-1 guides spinal commissural axons by activating its receptor DCC (Deleted in Colorectal Cancer). We have found that chemical inhibitors of metalloproteases potentiate netrin-mediated axon outgrowth *in vitro*. We have also found that DCC is a substrate for metalloprotease-dependent ectodomain shedding, and that the inhibitors block proteolytic processing of DCC and cause an increase in DCC protein levels on axons within spinal cord explants. Thus, potentiation of netrin activity by inhibitors may result from stabilization of DCC on the axons, and proteolytic activity may regulate axon migration by controlling the number of functional extracellular axon guidance receptors.

There is evidence that proteolytic activity present on neuronal growth cones may regulate their migratory activity (1). This possibility is supported by the presence of axonal stalling defects in flies with mutations in the *kuzbanian* gene, which encodes a member of the ADAM class of metalloproteases (2). ADAM class metalloproteases are also implicated in other biological processes, including fertilization (3), lateral inhibition during neurogenesis (4), and protein ectodomain shedding of a variety of ligands and receptors [(5–7), reviewed in (5)].

The netrin-1 protein and its receptor, DCC, are required for commissural axon outgrowth *in vitro* and for the proper guidance of spinal commissural neurons *in vivo* (8–12). We previously characterized an unidentified proteinaceous activity, termed netrin-synergizing activity (NSA), that potentiates the axon out-

growth-promoting effects of netrin on rat E11 (embryonic day 11) dorsal spinal cord explants (7, 13). In a screen of several dozen known molecules (including many axon guidance molecules), none could potentiate netrin activity (13). Upon further screening, we found that netrin-1 activity was potentiated by IC-3, a specific hydroxamate inhibitor of metalloproteases (6, 14) (Fig. 1). In the absence of any factors, or in the presence of a low concentration of netrin-1 (~50 ng/ml), very little outgrowth was observed from these explants (Fig. 1, A and B). Robust outgrowth was observed from explants grown in the presence of both 40 µM IC-3 and netrin-1 (~50 ng/ml) (Fig. 1D), which was greater than that observed with a high concentration of netrin-1 (1 µg/ml) alone (Fig. 1E). In contrast, much less outgrowth was observed from explants grown in the presence of 40 µM IC-3 alone (Fig. 1C); the fact that any outgrowth was observed may reflect a potentiation of low levels of endogenous netrin-1 present in dorsal regions of the spinal cord (9). The responsive axons in these assays are commissural, as assessed by expression of the commissural axon markers TAG-1 and DCC (15).

The degree of outgrowth observed in the presence of both IC-3 and netrin-1 (thick and long axon fascicles emerging primarily but not exclusively from the ventral cut edge of the explants) was similar to that observed with netrin-1 and NSA (8, 13). Quantification of axonal outgrowth (estimated as total axonal length) with IC-3 alone or IC-3 plus netrin-1 (Fig. 1F) revealed peak activity of IC-3 at 80 µM, and only slight activity at 20 µM.

The effect of IC-3 is likely to be due to its metalloprotease inhibitor activity because this compound has not been found to have any effect other than metalloprotease inhibition in a wide variety of cellular assays (including protein phosphorylation and cell viability) or in mice (14). To confirm this, we also compared the actions of a chemically distinct hydroxamate metalloprotease inhibitor, GM6001, and an inactive control isomer of this compound (16). As expected, GM6001 but not the control isomer showed a similar potentiation of netrin-1 activity to IC-3 (15), consistent with the potentiation of netrin-1 being due to inhibition of metalloprotease activity. Members of another class of inhibitors that function through chelation of the divalent cations required for metalloprotease function (including 1,10-phenanthroline and EDTA) could not be tested in these assays because they were toxic to the explants (15).

Dorsal spinal cord explants grown in the presence of IC-3 exhibited much brighter staining for DCC than did control axons grown in the absence of any factors (compare Fig. 2, C and D). This effect was specific for DCC, because explants grown with or without IC-3 and stained for TAG-1 exhibited no clear difference in staining intensity except at the ventral cut edge of the explant (Fig. 2, A and B). Quantification of fluorescence intensity across the dorsoventral axis of DCC-stained explants revealed an increase over almost the entire dorsoventral length of the explants (Fig. 2E).

Because IC-3 increased DCC staining levels within dorsal spinal cord explants, we tested whether DCC might be a substrate for

Department of Anatomy, Howard Hughes Medical Institute, and Department of Biochemistry and Biophysics, University of California, San Francisco, CA 94143, USA.

\*To whom correspondence should be addressed. E-mail: marctl@itsa.ucsf.edu